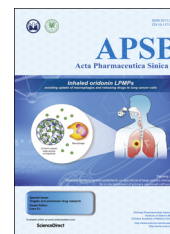




Chinese Pharmaceutical Association
Institute of Materia Medica, Chinese Academy of Medical Sciences

Acta Pharmaceutica Sinica B

www.elsevier.com/locate/apsb
www.sciencedirect.com



ORIGINAL ARTICLE

Euphorbia factor L2 induces apoptosis in A549 cells through the mitochondrial pathway



Minting Lin^a, Sili Tang^a, Chao Zhang^a, Hubiao Chen^b,
Wenjing Huang^a, Yun Liu^a, Jianye Zhang^{a,*}

^aSchool of Pharmaceutical Sciences, Guangzhou Medical University, Guangzhou 510182, China

^bSchool of Chinese Medicine, Hong Kong Baptist University, Hong Kong, China

Received 15 March 2016; received in revised form 20 May 2016; accepted 8 June 2016

KEY WORDS

Euphorbia Factor L2;
Caper euphorbia seed;
Euphorbia lathyris L.;
Anticancer agent;
Apoptosis;
Mitochondrial pathway

Abstract Euphorbia factor L2, a lathyran diterpenoid isolated from caper euphorbia seed (the seeds of *Euphorbia lathyris* L.), has been traditionally applied to treat cancer. This article focuses on the cytotoxic activity of Euphorbia factor L2 against lung carcinoma A549 cells and the mechanism by which apoptosis is induced. We analyzed the cytotoxicity and related mechanism of Euphorbia factor L2 with an MTT assay, an annexin V-FITC/PI test, a colorimetric assay, and immunoblotting. Euphorbia factor L2 showed potent cytotoxicity to A549 cells. Euphorbia factor L2 led to an increase in reactive oxygen species (ROS) generation, a loss of mitochondrial electrochemical potential, release of cytochrome *c*, activation of caspase-9 and caspase-3, and cleavage of poly(ADP-ribose) polymerase, suggesting that Euphorbia factor L2 induced apoptosis through a mitochondrial pathway. The cytotoxic activity of Euphorbia factor L2 in A549 cells and the related mechanisms of apoptotic induction provide support for the further investigation of caper euphorbia seeds.

© 2017 Chinese Pharmaceutical Association and Institute of Materia Medica, Chinese Academy of Medical Sciences. Production and hosting by Elsevier B.V. This is an open access article under the CC BY-NC-ND license (<http://creativecommons.org/licenses/by-nc-nd/4.0/>).

*Corresponding author.

E-mail address: jianyez@163.com (Jianye Zhang).

Peer review under responsibility of Institute of Materia Medica, Chinese Academy of Medical Sciences and Chinese Pharmaceutical Association.

1. Introduction

Lung cancer is the leading cause of cancer-related mortality in the world and non-small-cell lung cancer (NSCLC) is the most common form of lung cancer^{1,2}. Cancer chemotherapy has been regarded as one of the most effective therapy and the development of new anticancer agents is a promising strategy to treat cancer. Indeed, a growing body of evidence suggests that the success of anticancer chemotherapy depends on the discovery of novel anticancer agents³.

Traditional Chinese medicine provides a rich resource in the search for novel anticancer agents, of which caper euphorbia seed has been recorded for treating cancer⁴. The genus *Euphorbia* (spurges, Euphorbiaceae) has received worldwide attention as its exceptional diversity of growth forms and near-worldwide distribution⁵. It is the largest genus in the spurge family (Euphorbiaceae), containing more than 2000 species. The seeds of *Euphorbia lathyris* L. (caper euphorbia seed) have been used medicinally for the treatment of hydropsy, ascites, terminal schistosomiasis, and snakebites⁶. What's more, the seeds of *E. lathyris* L. can be used for cancer treatment⁷.

Multidrug resistance (MDR) is the major impediment to the efficient treatment of tumors. Previous studies revealed that lathyrane diterpenes extracted from the seeds of *E. lathyris* L., *Euphorbia* factor L1–L11 (EFL1–11), have been considered as promising P-glycoprotein (P-gp) modulators in MDR-mediated resistance^{8,9}. We have reported the isolation, identification and anticancer activity of EFL1¹⁰. On that basis, we further isolated EFL2 (Fig. 1A), and identified the structure using ¹H and ¹³C NMR, DEPT and high resolution electrospray ionization mass spectrometry (HR-ESI-MS). The structure was also reported by Appendino and co-workers¹¹ from the same plant species. In this study, we elucidated the mechanism of EFL2 cytotoxicity against the lung cancer cell line A549. Our results reveal that EFL2 does show potent cytotoxicity and induces apoptosis *via* a mitochondrial pathway in A549 cells.

2. Materials and methods

2.1. Chemicals and reagents

EFL2 was isolated from the seeds of *E. lathyris* L. with a purity of more than 98%. 3-(4,5-Dimethyl-2-thiazoly)2,5-diphenyl-2H-tetrazolium bromide (MTT), 2',7'-dichlorofluorescein diacetate (DCFH-DA), 3,3'-dihexyloxycarbocyanine iodide (DiOC₆) were obtained from Sigma Chemical Co. (USA). Primary antibodies were obtained as follows: antibodies against GAPDH, anti-mouse IgG-HRP and anti-

rabbit IgG-HRP from KangChen Biotechnology Co. (Shanghai, China), antibody against cytochrome *c* from Santa Cruz Biotechnology Co. Colorimetric assay kits for caspase-9 and caspase-3 were purchased from R&D systems (Minneapolis, MN, US). All tissue culture supplies were products of Life Technologies. Other routine laboratory reagents were obtained from commercial sources of analytical or HPLC grade.

2.2. Cell lines and cell culture

Lung cancer A549 cells were maintained in RPMI 1640 medium containing 100 U/mL penicillin, 100 μmol/L streptomycin, and 10% fetal bovine serum (FBS). Cells were cultured in a humidified atmosphere incubator of 5% CO₂ at 37 °C¹².

2.3. Cell viability assay

The effect of EFL2 on cell viability was detected by MTT assay. Cells were harvested and transferred into 96-well plates at a density of 5 × 10⁴ cells/mL. After 24 h incubation, 10 μL EFL2 solution (0, 4.162, 6.243, 9.364, 14.05, 21.07, 31.60, 47.41, 71.11, 106.7, 160 and 240 μmol/L) was added to 96-well plates. After 68 h of treatment, 10 μL MTT (10 mmol/L stock solution in saline) was added to each well and incubated in darkness for 4 h at 37 °C. Subsequently, the supernatant was removed and 100 μL anhydrous dimethyl sulfoxide was added into each well. Cell viability was measured with a Model 550 Microplate reader (BIO-RAD, USA) at 540 nm and 655 nm as reference filter. The growth-inhibitory effect of EFL2 was expressed as IC₅₀ estimated from the concentration–response curve (Bliss's software). Cell survival was calculated using the following formula¹³: Survival (%) = (Mean experimental absorbance / Mean control absorbance) × 100.

2.4. Annexin V-FITC/PI assay for apoptosis

Apoptosis was quantified by measuring surface exposure of phosphatidylserine in apoptotic cells using an annexin V-FITC/PI (propidium iodide) apoptosis detection kit (KeyGEN Biotech, Nanjing, China) according to the manufacturer's protocol. Briefly, after A549 cells were treated with the indicated concentrations (40 and 80 μmol/L) of EFL2 for 48 h, the cells were collected and washed twice with ice-cold phosphate-buffered saline (PBS). Then 5 × 10⁵ cells were resuspended with 0.5 mL binding buffer containing Annexin-V (1:50 according to the manufacturer's instruction) and 40 ng/sample of PI for 30 min at 37 °C in the dark. Subsequently, the cells were assayed by flow cytometer

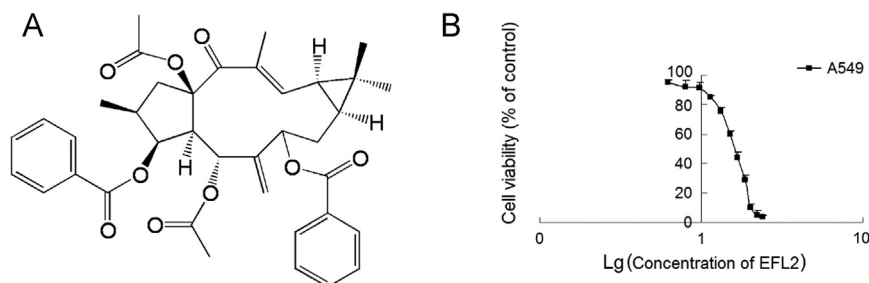


Figure 1 Structure of EFL2 and its cytotoxicity to A549 cells. (A) Chemical structure of Euphorbia factor L2 (EFL2); (B) EFL2 inhibited viability of A549 cells with log scale of concentration.

(Becton Dickinson, USA) and analyzed with the CellQuest software (Becton Dickinson, USA). At least 10,000 cells were analyzed for each sample. The apoptosis rate was calculated using the following formula¹⁴: Apoptosis rate (%) = (Number of apoptotic cells/Number of total cells observed) × 100.

2.5. Measurement of ROS generation

The fluorescence intensity of 2',7'-dichlorofluorescein (DCF) is proportional to the amount of reactive oxygen species (ROS) produced by the cells. After exposure to the indicated concentrations (40 and 80 µmol/L) of EFL2 for 24 h, 5×10^5 cells were harvested, washed with PBS and incubated with DCFH-DA (50 µmol/L in a final concentration) at 37 °C for 20 min in the dark. Then the cells were washed twice and resuspended in 1 mL PBS. ROS generation was determined from 10,000 cells in each sample by FACS (fluorescence-activated cell sorting) with a Caliber flow cytometer (Beckman-coulter, Elite) at the excitation wavelength of 488 nm and emission wavelength of 530 nm. The data were analyzed by CellQuest software (Becton Dickinson, USA) and expressed as median fluorescence intensity (MFI)¹⁵.

2.6. Determination of mitochondrial membrane potential ($\Delta\Psi_m$)

A549 cells (5×10^5 cells/mL) were treated with EFL2 at the indicated concentrations (40 and 80 µmol/L) for 24 h to determine $\Delta\Psi_m$. The cells were collected, centrifuged at 600g for 5 min, and washed with PBS. Thereafter cells were incubated with 40 nmol/L DiOC₆(3) at 37 °C for 20 min in the dark. Subsequently, the stained cells were washed twice with chilled PBS prior to suspension in 1 mL PBS, and then the amount of DiOC₆(3) retained by 10,000 cells per sample was analyzed by FASCanto Flow Cytometer (Beckman Coulter Inc., USA) with the excitation wavelength of 484 nm and emission wavelength of 501 nm. The data obtained from flow cytometry were analyzed with CellQuest software (Becton Dickinson, USA) and expressed as MFI¹⁶.

2.7. Activities measurement of caspase-9 and caspase-3 by colorimetric assay

The activities of caspase-9 and caspase-3 were measured with a caspase colorimetric assay kit according to the manufacturer's protocol. Briefly, 1×10^6 cells were treated with 80 µmol/L EFL2 for 12, 24, 36 or 48 h. Subsequently, cells were collected, washed with ice-cold PBS and lysed in lysis buffer. The lysates were assayed for protease activity with the caspase-specific peptide conjugated with the color reporter molecule *p*-nitroanaline. The chromophore *p*-nitroanaline cleaved by caspases was quantified with the spectrophotometer at a wavelength of 405 nm. The caspase enzymatic activities in cell lysates were proportional to the color intensity¹¹.

2.8. Western blot analysis of cytosolic cytochrome *c*, caspase-9, caspase-3 and PARP

Expression of cytochrome *c*, caspase-9, caspase-3, and poly (ADP-ribose) polymerase (PARP) was detected by Western blot analysis as previously reported¹⁷. Approximately 3.5×10^6 – 4.0×10^6 cells/well were seeded into culture dishes, incubated with 80 µmol/L EFL2 for 0, 12, 24, 48 h and then washed with ice-cold PBS.

For whole cell lysates, the pellet was lysed in $1 \times$ loading buffer [50 mmol/L Tris-HCl (pH 6.8); 10% glycerol, *v/v*; 2% sodium

dodecylsulphate, *w/v*; 0.25% bromphenol blue, *w/v*; 0.1 mol/L D,L-dithiothreitol (DTT)]. After treatment at 100 °C for 20 min, the lysates were centrifuged and the supernatant was collected¹⁸.

For subcellular fractionation of cytosol, cells were harvested and resuspended in a 5-fold volume of ice-cold cell extract buffer [20 mmol/L HEPES-KOH (pH 7.5), 10 mmol/L KCl, 1.5 mmol/L MgCl₂, 1 mmol/L EDTA, 1 mmol/L EGTA, 1 mmol/L DTT, 250 mmol/L sucrose, 0.1 mmol/L phenylmethanesulfonyl fluoride (PMSF) and 0.02 mmol/L aprotinin] at 4 °C for 40 min. Then, the final supernatant after repeated centrifugation was collected and dissolved in $5 \times$ loading buffer [250 mmol/L Tris-HCl (pH 6.8); 50% glycerol, *v/v*; 10% sodium dodecylsulphate, *w/v*; 1.25% bromphenol blue, *w/v*; 0.5 mol/L DTT]. The samples were heated at 100 °C for 15 min and subjected to Western blot analysis. Equal amounts of protein were loaded onto 8%–12% sodium SDS-PAGE and transferred to PVDF membranes (Millipore, USA) and the membranes were incubated with specific primary antibodies. Proteins were then visualized using HRP-conjugated secondary antibody and a PhototopeTM-HRP detection kit (Cell Signaling, USA) on Kodak medical X-ray processor (Kodak, USA). The cytochrome *c* protein was detected by anti-cytochrome *c* antibody in a ratio of 1:1000^{19,20}.

2.9. Statistical analysis

Results were analyzed by *t*-test or one-way ANOVA with SPSS 13.0 software (SPSS Inc., USA). Data are presented as mean ± SD of at least triplicate determinations. **P* < 0.05 and ***P* < 0.01 were considered significant differences.

3. Results

3.1. EFL2 exerted potent cytotoxicity against A549 cells

The cytotoxicity of EFL2 was measured by MTT assay. The IC₅₀ of EFL2 was 36.82 ± 2.14 µmol/L for A549 cells (Fig. 1B), suggesting that EFL2 exhibited potent cytotoxicity to A549 cells.

3.2. EFL2-induced cell apoptosis in A549 cells

To explore whether the anti-tumor effect of EFL2 on A549 cells was associated with apoptosis induction, the cells were treated with 40 and 80 µmol/L of EFL2 for 48 h and apoptosis was monitored by flow cytometry following annexin V and PI staining. The results showed that apoptosis rates were $6.2 \pm 1.5\%$, $23.7 \pm 3.4\%$, $36.9 \pm 2.4\%$ for control, 40 and 80 µmol/L EFL2, respectively (Fig. 2).

3.3. EFL2-induced increase of intracellular ROS levels in A549 cells

It is well-known that an increase in intracellular ROS can lead to apoptosis²¹. For this purpose, the generation of ROS was assessed by a flow cytometric method with DCFH-DA used as the fluorescent probe. After A549 cells were exposed to 40 and 80 µmol/L EFL2 for 24 h, the intracellular ROS levels were $266.23 \pm 38.53\%$ and $363.64 \pm 40.26\%$ of control, respectively (Fig. 3). These results imply that EFL2 might cause the loss of $\Delta\Psi_m$ via ROS, which was subsequently shown by mitochondrial membrane-potential assay.

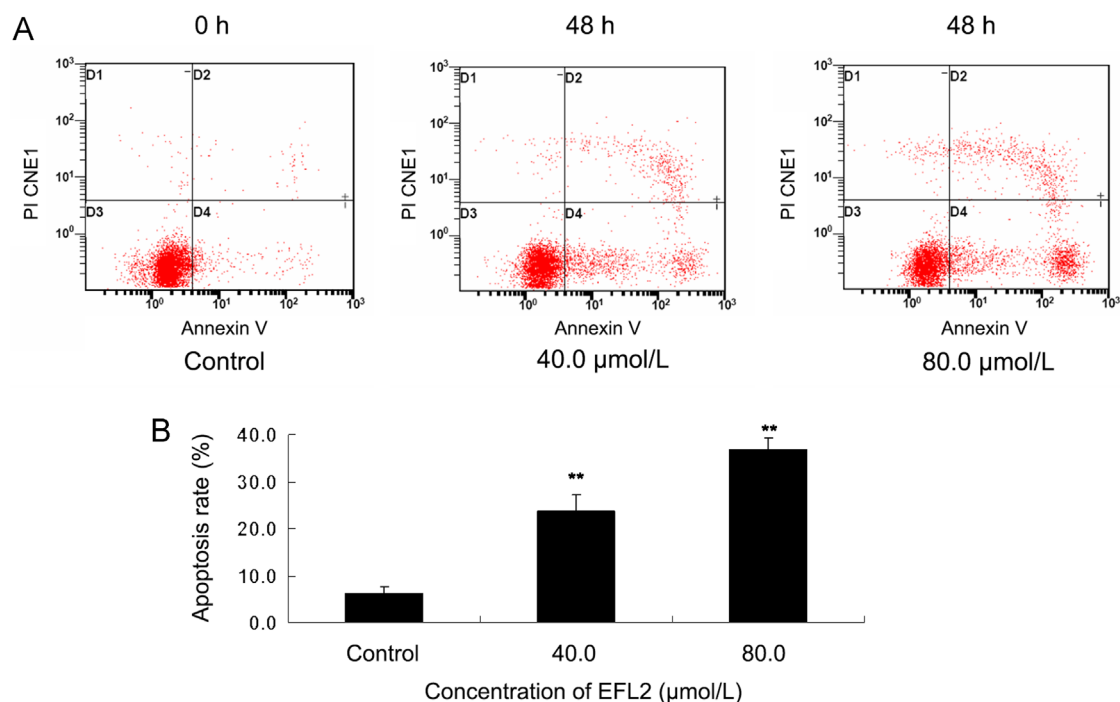


Figure 2 EFL2-induced cell apoptosis in A549 cells. (A) A549 cells were treated with 0, 40 and 80 μmol/L of EFL2 for 48 h, apoptosis rates were then detected by annexin V-FITC/PI double staining and flow cytometer. D4 quadrant represented cells stained mainly by annexin-V (early apoptotic cells) and D2 quadrant represented cells stained by both PI and annexin-V (late apoptotic). D1 quadrant represented cells stained mainly by PI and viable cells negative for both annexin-V and PI appeared in the D3 quadrant. (B) The apoptosis rate was showed in the bar graph.

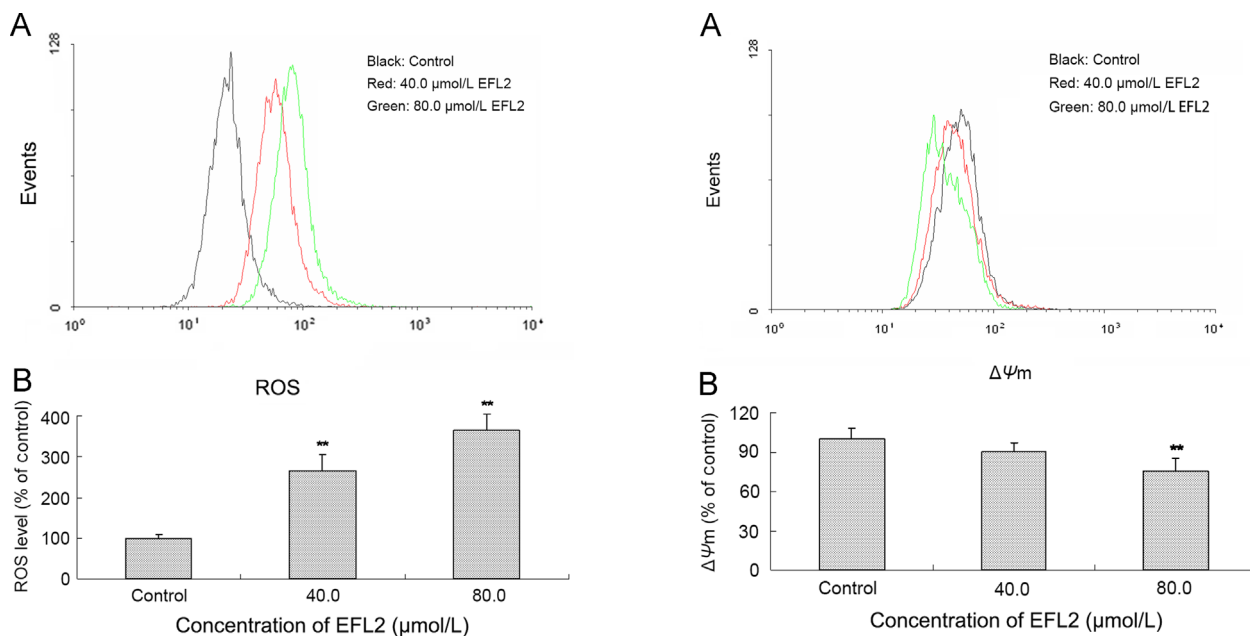


Figure 3 EFL2 increased ROS levels in A549 cells. (A) ROS generation was increased in A549 cells; (B) ROS levels in A549 cells were calculated as percentage of control.

3.4. EFL2-induced loss of mitochondrial membrane potential ($\Delta\Psi_m$) in A549 cells

Apoptosis is a complex and multifactorial process in which mitochondria are involved. Generally, generation of ROS induced by chemotherapeutic drugs would trigger mitochondrial

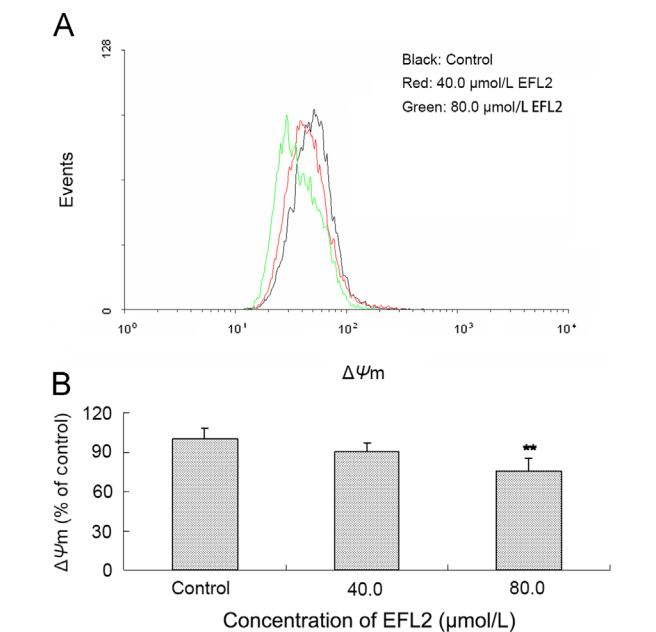


Figure 4 EFL2 decreased $\Delta\Psi_m$ in A549 cells. (A) The decrease of $\Delta\Psi_m$ level was observed in A549 cells; (B) $\Delta\Psi_m$ level in A549 cells was calculated as percentage of control.

pathway, leading to the loss of $\Delta\Psi_m$ ²². To investigate the mechanisms of EFL2-induced apoptosis in A549 cells, the effects of EFL2 on $\Delta\Psi_m$ were determined by flow cytometric analysis. After A549 cells were treated with the indicated concentrations of EFL2 for 24 h, the decrease in $\Delta\Psi_m$ was observed in a concentration-dependent manner (Fig. 4). After treatment, the

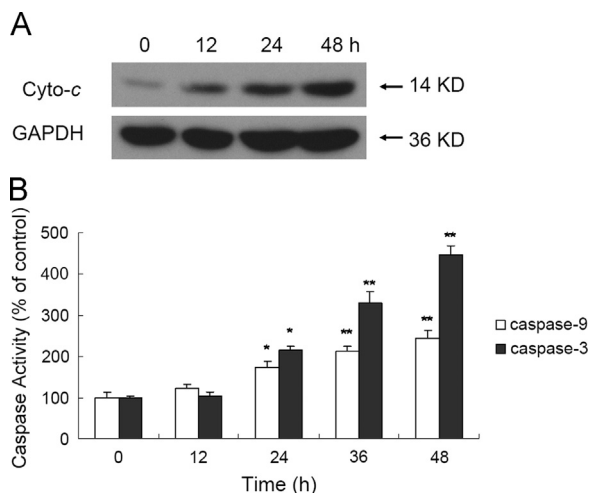


Figure 5 EFL2 activates the expression of cytochrome *c* in A549 cells. (A) Release of cytochrome *c* was discovered in A549 cells; (B) activation of caspase-9 and caspase-3 were detected in A549 cells.

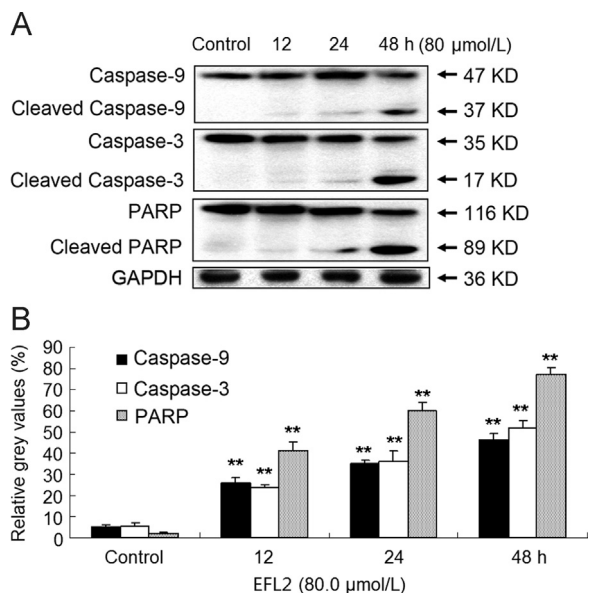


Figure 6 EFL2 activates the expression of caspase-9 and caspase-3, and the cleavage of PARP in A549 cells in a time-dependent manner. (A) Activation of caspase-9 and caspase-3, and the cleavage of PARP were detected in A549 cells; (B) densitometric analysis of Western blot results of (A). The molecular weight of activated (cleaved) caspase-9, caspase-3 and cleaved PARP were 37, 17 and 89 kD, respectively. GAPDH (36 kD) was used to confirm equal protein loading. Results were expressed as mean \pm SD of at least three determinations.

$\Delta\Psi_m$ was $90.39 \pm 6.91\%$ and $75.47 \pm 9.35\%$ of control for 40 and 80 $\mu\text{mol/L}$ EFL2, respectively. These data indicate that mitochondrial dysfunction is involved in the apoptosis induced by EFL2.

3.5. EFL2-induced release of cytochrome *c*

The increase in intracellular ROS and loss of $\Delta\Psi_m$ have been demonstrated to cause the release of cytochrome *c*. The release of cytochrome *c* from mitochondria into the cytosol is a vital factor in

the mitochondrial pathway of apoptosis. In this regard, Western blot analysis was used to determine the cytosolic levels of cytochrome *c*. After A549 cells were treated with 80 $\mu\text{mol/L}$ EFL2 for indicated time, the release of cytochrome *c* was detected in A549 cells (Fig. 5A).

3.6. EFL2 activated the expression of caspase-9 and caspase-3, and the cleavage of PARP

After release of cytochrome *c*, the caspase cascade would subsequently be activated. For this, the activation of caspase-9 and caspase-3, and the cleavage of PARP were measured in A549 cells (Figs. 5B and 6). After A549 cells were incubated with 80 $\mu\text{mol/L}$ apicidin for 0, 12, 24, 48 h, cells were harvested and Western blot analysis was used to determine relative levels of each protein. Densitometric ratios of cleaved caspase-9 were $5.33 \pm 0.72\%$, $26.06 \pm 2.36\%$, $35.10 \pm 1.72\%$ and $46.51 \pm 2.83\%$, at the respective time-points. Densitometric ratios of cleaved caspase-3 were $5.51 \pm 1.47\%$, $23.68 \pm 1.15\%$, $35.99 \pm 5.30\%$ and $52.04 \pm 3.29\%$, respectively. Densitometric ratios of cleaved PARP were $2.01 \pm 0.42\%$, $41.24 \pm 4.11\%$, $59.76 \pm 4.07\%$ and $77.51 \pm 2.86\%$, respectively.

Taken together, EFL2 led to an increase in ROS generation, a loss of mitochondrial potential, release of cytochrome *c*, activation of caspase-9 and caspase-3, and the cleavage of PARP, which suggests that EFL2-induced apoptosis of A549 cells through a mitochondrial pathway.

4. Discussion

Lung cancer continues to be the most common cause of cancer-related mortality worldwide, killing more people than prostate, breast, pancreas and colon cancers combined²³. The trend in five-year relative survival rates of lung cancer patients is only 15%. Although some therapeutic advances have been achieved, such as chemotherapy that provides useful palliation, therapies for advanced lung cancer are far from satisfactory. A major problem in the treatment of lung cancer is the MDR. Thus, novel approaches to enhance the antitumorigenic effects of chemotherapeutic agents are required²⁴. Numerous natural cancer chemopreventive agents have already been isolated and are being used for the treatment of cancers.

Recent research has revealed that herbal medicines and natural products isolated from plants could provide additional strategies for monotherapy or combination treatments. EFL2 was isolated from the seeds of *E. lathyris* L. (Caper Euphorbia Seed). Our study showed that it was able to inhibit the growth of human lung cancer A549 cells potently with an IC_{50} value of $36.82 \pm 2.14 \mu\text{mol/L}$. Herein, we carried out further investigations to elucidate the mechanisms involved.

As is well known, many chemotherapeutic drugs act by inducing apoptosis. The apoptotic mechanism of cancer cells is composed of both upstream regulators and downstream effector components. The regulators can be divided into two major circuits. One receives and processes extracellular death-inducing signals which involve the Fas ligand/Fas receptor (the extrinsic apoptotic program). The other senses and integrates a variety of signals of intracellular origin (the intrinsic program). Each culminates in the activation of caspases-8 and caspases-9, respectively. As to the activation of protease, a cascade of proteolysis of effector caspases directly responsible for the execution phase of apoptosis is activated. In this way, the cancer cells are progressively disassembled and then consumed both by neighboring cells and

phagocytic cells. Currently, the intrinsic apoptotic mechanism is more widely implicated in cancer pathogenesis^{22,25}.

Indeed, release of cytochrome *c* and activation of caspase-9 and caspase-3 in time-dependent manner were observed in A549 cells after exposure to EFL2 (Figs. 5 and 6). Caspase activity measured by colorimetric assay (Fig. 5B) was essentially in agreement with results obtained by Western blot (Fig. 6). What's more, the cleavage of PARP was detected in our experiments (Fig. 6). Taken together, EFL2 induced apoptosis of A549 *via* a mitochondrial pathway.

Generally, loss of mitochondrial membrane potential ($\Delta\Psi_m$) is involved in the mitochondrial pathway. Consistently, $\Delta\Psi_m$ of A549 was decreased after treatment with EFL2 for 24 h showing concentration-dependent pattern (Fig. 4). Furthermore, an increase of ROS was noted (Fig. 3), which could cause the loss of $\Delta\Psi_m$.

5. Conclusions

In summary, our study shows that the anticancer activity of EFL2 against lung cancer A549 cells involves mitochondrially-mediated apoptosis, and provides evidence for the further investigation of caper euphorbia seed.

Acknowledgments

The work was supported by National Natural Science Foundation of China (No. 81473320), Fund from Guangdong Science and Technology Department & Guangdong Academy of Traditional Chinese Medicine (2016A020226024), Fund of Guangdong Education Department (2015KTSCX112), the Science Fund of the Education Bureau of Guangzhou City (1201410039 and 2012C208).

References

- Xiao X, Yu SR, Li SC, Wu JZ, Ma R, Cao HX, et al. Exosomes: decreased sensitivity of lung cancer A549 cells to cisplatin. *PLoS One* 2014;**9**:e89534.
- Jing W, Li M, Zhang Y, Teng F, Han A, Kong L, et al. PD-1/PD-L1 blockades in non-small-cell lung cancer therapy. *Onco Targets Ther* 2016;**9**:489–502.
- Li L, Leung PS. Use of herbal medicines and natural products: an alternative approach to overcoming the apoptotic resistance of pancreatic cancer. *Int J Biochem Cell Biol* 2014;**53**:224–36.
- Hong SH, Ismail IA, Kang SM, Han DC, Kwon BM. Cinnamaldehydes in cancer chemotherapy. *Phytother Res* 2016;**30**:754–67.
- Ernst M, Grace OM, Saslis-Lagoudakis CH, Nilsson N, Simonsen HT, Rønsted N. Global medicinal uses of *Euphorbia* L. (Euphorbiaceae). *J Ethnopharmacol* 2015;**176**:90–101.
- Lu J, Li GY, Huang J, Zhang C, Zhang L, Li P, et al. Lathyrane-type diterpenoids from the seeds of *Euphorbia lathyris*. *Phytochemistry* 2014;**104**:79–88.
- Itokawa H, Ichihara Y, Watanabe K, Takeya K. An antitumor principle from *Euphorbia lathyris*. *Planta Med* 1989;**55**:271–2.
- Vieira C, Duarte N, Reis MA, Spengier G, Madureira AM, Molnár J, et al. Improving the MDR reversal activity of 6,17-epoxylathyrane diterpenes. *Bioorg Med Chem* 2014;**22**:6392–400.
- Reis MA, Paterna A, Mónico A, Molnar J, Lage H, Ferreira MJ. Diterpenes from *Euphorbia piscatoria*: synergistic interaction of lathyranes with doxorubicin on resistant cancer cells. *Planta Med* 2014;**80**:1739–45.
- Zhang JY, Zhang C, Chen HB, Fu LW, Tao YW, Zheng XQ, et al. Assignments of ¹H and ¹³C NMR signals of euphorbia factor L1 and investigation of its anticancer activity *in vitro*. *J Med Plants Res* 2010;**4**:335–8.
- Appendino G, Tron GC, Cravotto G, Palmisano G, Jakupovic J. An expeditious procedure for the isolation of ingenol from the seeds of *Euphorbia lathyris*. *J Nat Prod* 1999;**62**:76–9.
- Zhang JY, Tao LY, Liang YJ, Yan YY, Dai CL, Xia XK, et al. Secalonic acid D induced leukemia cell apoptosis and cell cycle arrest of G1 with involvement of GSK-3 β /catenin/c-Myc pathway. *Cell Cycle* 2009;**8**:2444–50.
- Zhang JY, Lin MT, Tung HY, Tang SL, Yi T, Zhang YZ, et al. Bruceine D induces apoptosis in human chronic myeloid leukemia K562 cells *via* mitochondrial pathway. *Am J Cancer Res* 2016;**6**:819–26.
- Fallahian F, Aghaei M, Abdolmohammadi MH, Hamzeloo-Moghadam M. Molecular mechanism of apoptosis induction by gaillardin, a sesquiterpene lactone, in breast cancer cell lines: gaillardin-induced apoptosis in breast cancer cell lines. *Cell Biol Toxicol* 2015;**31**:295–305.
- Wang XH, Jia DZ, Liang YJ, Yan SL, Ding Y, Chen LM, et al. Lgf- γ L-9 induces apoptosis in human epidermoid carcinoma KB cells and multidrug resistant KBv200 cells *via* reactive oxygen species-independent mitochondrial pathway. *Cancer Lett* 2007;**249**:256–70.
- He LW, Han JJ, Li BW, Huang L, Ma K, Chen Q, et al. Identification of a new cyathane diterpene that induces mitochondrial and autophagy-dependent apoptosis and shows a potent *in vivo* anticancer activity. *Eur J Med Chem* 2016;**111**:183–92.
- Zhang JY, Wu HY, Xia XK, Liang YJ, Yan YY, She ZG, et al. Anthracenedione derivative 1403P-3 induces apoptosis in KB and KBv200 cells *via* reactive oxygen species-independent mitochondrial pathway and death receptor pathway. *Cancer Biol Ther* 2007;**6**:1413–21.
- Tao YW, Lin YC, She ZG, Lin MT, Chen PX, Zhang JY. Anticancer activity and mechanism investigation of beauvericin isolated from secondary metabolites of the mangrove endophytic fungi. *Anti-Cancer Agents Med Chem* 2015;**15**:258–66.
- Liu XD, Fan RF, Zhang Y, Yang HZ, Fang ZG, Guan WB, et al. Down-regulation of telomerase activity and activation of caspase-3 are responsible for tanshinone I-induced apoptosis in monocyte leukemia cells *in vitro*. *Int J Mol Sci* 2010;**11**:2267–80.
- Gao S, Liu HY, Wang YH, He HP, Wang JS, Di YT, et al. Lathyranone A: a diterpenoid possessing an unprecedented skeleton from *Euphorbia lathyris*. *Org Lett* 2007;**9**:3453–5.
- Xie FF, Pan SS, Ou RY, Zheng ZZ, Huang XX, Jian MT, et al. Volasertib suppresses tumor growth and potentiates the activity of cisplatin in cervical cancer. *Am J Cancer Res* 2015;**5**:3548–59.
- Hanahan D, Weinberg RA. Hallmarks of cancer: the next generation. *Cell* 2011;**144**:646–74.
- Zhao J, Li QQ, Zou B, Wang G, Li X, Kim JE, et al. *In vitro* combination characterization of the new anticancer plant drug β -elemene with taxanes against human lung carcinoma. *Int J Oncol* 2007;**31**:241–52.
- Li L, Xu L, Qu X, Zhao M, Yu P, Kang J, et al. Cbl-regulated Akt and ERK signals are involved in β -elemene-induced cell apoptosis in lung cancer cells. *Mol Med Rep* 2011;**4**:1243–6.
- Choi JH, Lee JY, Choi AY, Hwang KY, Choe W, Yoon KS, et al. Apicidin induces endoplasmic reticulum stress- and mitochondrial dysfunction-associated apoptosis *via* phospholipase C γ 1- and Ca²⁺-dependent pathway in mouse Neuro-2a neuroblastoma cells. *Apoptosis* 2012;**17**:1340–58.